Electronic Supplementary Material (ESI) for RSC Advances.

New exploration towards the dinuclear Iridium(II) complexes materials under chlorine-bridged precursor

Ming-Xing Song,[a] Yuan Li,[b] Duo Xu,[a] Rui-Ping Deng,[c] Fu-Quan Bai[b]† and Zheng-Kun Qin[a]†

[a.] *College of Information Technology, Jilin Normal University, Siping 136000, People's Republic of China.*

[b.] *Institute of Theoretical Chemistry, Jilin University, Changchun 130023, China.*

[c.] *State Key Laboratory of Rare Earth Resource Utilization, Changchun Institute of Applied Chemistry, Chinese Academy of Sciences, 5625 Renmin Street, Changchun 130022, People's Republic of China.*

† Corresponding author: Fu-Quan Bai (Email: baifq@jlu.edu.cn) and Zheng-Kun Qin (Email: qin_zhengkun@126.com).

Experimental Section

All solvents were of analytical reagent grade and purified according to standard procedures. Ppy, dfppy, $[\{Ir(ppy)_2Cl\}_2]$ and $[\{Ir(dfppy)_2Cl\}_2]$ was synthesized according to a process which is similar to the reported literature. Other reagents were purchased commercially and used without further purification.

Synthesis of 2-phenylpyridine (ppy)

0.72 g (6.38 mmol) of phenylboronic acid and 0.9 g (5.74 mmol) of 2-bromopyridine were put into a mixture of 6 ml of toluene and 3 ml of ethanol, and the resultant solution was stirred. Then, 0.2 g (0.178 mmol) of tetrakis(triphenylphosphine)palladium^0 and 6 ml of 2M aqueous Na_2CO_3 solution were added to the above solution. The reaction mixture was reacted by refluxing while being stirred under a nitrogen atmosphere for five hours, and was cooled down to room temperature. The reaction solution was poured into water and extracted with ethyl acetate. Organic layers were dried with $MgSO_4$ and evaporated under a reduced pressure. The residue was then purified by column chromatography (n-hexane: EtOAc = 10: 1 as eluant), to obtain 0.648 g (70%) of 2-phenylpyridine as a pure product. **^{1}H NMR** (400 MHz, $CDCl_3$) δ 7.15-7.29 (m 1H), 7.34-7.55 (m, 3H), 7.68-7.80 (m, 2H), 7.92-8.04 (m. 2H), 8.65-8.74 (m, 1H). **MODI–TOF**: calculated [M^+] 155.0714; observed [M^+] 155.0746.

Synthesis of 2-(2, 4-difluorophenyl)pyridine (dfppy)

2-Bromopyridine (1 mL, 10.54 mmol), 2, 4-difluorophenylboronic acid (2 g, 12.7 mmol) and tetrakis(triphenylphosphine)palladium^0 (0.37 g, 0.31 mmol) were dissolved in 20 mL of THF in a round-bottomed flask. After 15 mL of aqueous 2M Na_2CO_3 was delivered, reaction mixture was heated at 70 °C for 1 day under a nitrogen atmosphere. The cooled mixture was poured into water, extracted with CH_2Cl_2 (30 mL × 3 times) and then dried over anhydrous magnesium sulfate. Finally silica column purification (n-hexane: EtOAc = 7: 1 as eluant) gave product (1.52 g, 7.95 mmol) in 75% yield. **^{1}H NMR** (400 MHz, $CDCl_3$) δ = 8.76 – 8.55 (m, 1H), 8.04 – 7.81 (m, 2H), 7.74 (d, J = 8.0 Hz, 1H), 7.48 – 7.25 (m, 1H), 7.22 – 6.95 ppm (m, 2H). **MODI–TOF**: calculated [M^+] 191.0544; observed [M^+] 191.0546.

Synthesis of $[\{Ir(ppy)_2Cl\}_2]$

$IrCl_3.2H_2O$ (0.776 g, 2.6 mmol) and ppy (1.532 g, 9.88 mmol) were dissolved in 40 mL 2-methoxyethanol: water(3:1, v/v) solution, and refluxed at 140 °C for 24 h under an atmosphere of N_2. After cooling to room temperature, yellow precipitate was filtered and washed with acetone: ethanol = 15 mL: 15mL. The washed product was dried under vacuum with a (1.078 g, mmol) 77% yield. **MODI-TOF**: calculated [M^+] 1072.1609; observed [M^+] 1072.1639.

Synthesis of $[\{Ir(dfppy)_2Cl\}_2]$

$IrCl_3.2H_2O$ (1.15 g, 3.44 mmol) and dfppy (2.95 g, 15.44 mmol) were dissolved in 16 mL 2-methoxyethanol: water (3:1, v/v), and refluxed at 140 °C for 20 h under an atmosphere of N_2. After cooling to room temperature, yellow precipitate was filtered and washed with acetone: ethanol = 15 mL: 15mL. The washed product was dried under vacuum with a (1.36 g, 1.12 mmol) 65% yield. **MODI-TOF**: calculated [M^+] 1216.0509; observed [M^+] 1216.0499.

Synthesis of $[\{Ir(ppy)_2\}_2Cl(BTA)]$------Complex 1

A mixture of $[\{Ir(ppy)_2Cl\}_2]$ (0.216 g, 0.2 mmol) and BTA (0.0357g, 0.3 mmol) in 15 mL MeOH/CH_2Cl_2 (1:2 v/v) was refluxed under nitrogen in the dark for 24 h. The light brown solution was then cooled to room temperature. Then the mixture is then distilled at reduced pressure to remove the solutions. Finally silica column purification (n-hexane: EtOAc = 5: 1 as eluant) gave product (0.124 g, 0.146 mmol) in 73% yield. The product was dissolved in EtOAc, and the filtrate was allowed to evaporate slowly at room temperature. After one week, yellow block crystals suitable for X-ray diffraction were isolated.

Synthesis of $[\{Ir(dfppy)_2\}_2Cl(BTA)]$------Complex 2

A mixture of $[\{Ir(dfppy)_2Cl\}_2]$ (0.57 g, 0.47 mmol) and BTA (0.0839g, 0.705 mmol) in 30 mL MeOH/CH_2Cl_2 (1:2 v/v) was refluxed under nitrogen in the dark for 24 h. Then the light brown solution was then cooled to room temperature. The mixture is then distilled at reduced pressure to remove the solutions. Finally silica column purification (n-hexane: CH_2Cl_2 = 3: 1 as eluant) gave product (0.331 g, 0.36 mmol) in 77% yield. The product was dissolved in CH_2Cl_2, and the filtrate was allowed to evaporate slowly at -4 °C. After ten days, yellow block crystals suitable for X-ray diffraction were isolated.

Computational Method

The ground-state geometry of the two complexes has been fully optimized in the absence of the counterion at the Density Functional Theory (DFT) level, starting from the X-ray structures. The chosen exchange correlation (XC) functional is the widely used B3LYP in view of its good compromise between accuracy and computational cost; the basis set for the description of the electrons of nonmetallic atoms is 6-31G, while the LANL2DZ basis set, which have been shown to provide accurate interpretation and predication for the transition metal complexes in numerous applications in our previous work. [1-4], has been used for iridium. The characterization of the nature of the lowest-lying singlet and triplet excited states involved in absorption and emission properties, respectively, relies on time-dependent density functional theory (TD-DFT) calculations performed on the basis of the ground-state geometry, using the same functional and basis set. Our approach is motivated by previous works showing its adequacy to describe the electronic and optical properties of iridium complexes and complexes with other metals. Note that these calculations neglect intersystem crossing processes mixing states of the singlet and triplet manifold. All calculations were performed with the Gaussian 09 package[5].

about the radiative decay, within the regime of Born-Oppenheimer approximation and perturbation theory, the excited triplet state is perturbed by various excited singlet states due to the spin-orbit interactions. The radiative decay rate constants (k_r) from T_m state to S_0 can be represented as the form,

$$k_r^{\alpha}\left(T_m \rightarrow S_0\right)=\frac{\eta^3}{1.5}E\left(T_m\right)^3\left\{\sum_n \frac{\left\langle T_m^{\alpha} \mid H_{SOC} \mid S_n\right\rangle}{E\left(S_n\right)-E\left(T_m\right)}\left(\frac{f_n}{E\left(S_n\right)}\right)^{\frac{1}{2}}\right\}^2$$

where the superscript α indicates the spin substate of the triplet excited state T_m(α = x, y, or z), and η represents refractive index of the medium and the vacuum permittivity. The medium is CH_3CN with the refractive index of 1.344 in the current system. $E(T_m)$ is the vertical excitation energy from T_m to S_0 transition, and $E(S_n)$ is the vertical excitation energy from S_n to S_0 transition. $<T_m^{\alpha}|H_{SOC}|S_n>$ represents the spin-orbit coupling (SOC) matrix element between T_m and S_n. H_{SOC} is the N-electron Hamiltonian operator. f_n is the oscillator strength.

According to Boltzmann statistics distribution, these triplet substates are assumed to be at thermal equilibrium because of the fast spin relaxation. In the high-temperature limit, the radiative decay rate constant of the transition from T_m to S_0 state is determined by the average of the k_r^{α} values written as the form.

$$k_r=\frac{1}{3}\sum_{\alpha}^{3}k_r^{\alpha}$$

The zero-field splitting (ZFS) is also an important parameter to evaluate the phosphorescent performance of transition metal complexes. The energy shift of these three spin triplet sublevels can be expressed the form,

$$\Delta \mathrm{E}\left(T_m^{\alpha}\right)=\sum_n \frac{\left|\left\langle T_m^{\alpha} \mid H_{SOC} \mid S_n\right\rangle\right|^2}{E\left(S_n\right)-E\left(T_m\right)}$$

where α denotes the three sublevels of T_m excited state perturbed by S_n excited state. In general, the $\Delta E(ZFS)$ parameter value is larger giving rise to more MLCT character of the coupling excited states and the stronger SOC between these involved states in some extents. However, when the energy shifts of all three substates are near-equal, $\Delta E(ZFS)$ values sometimes may be small even though the contribution of the metal centre in the complexes is large enough.

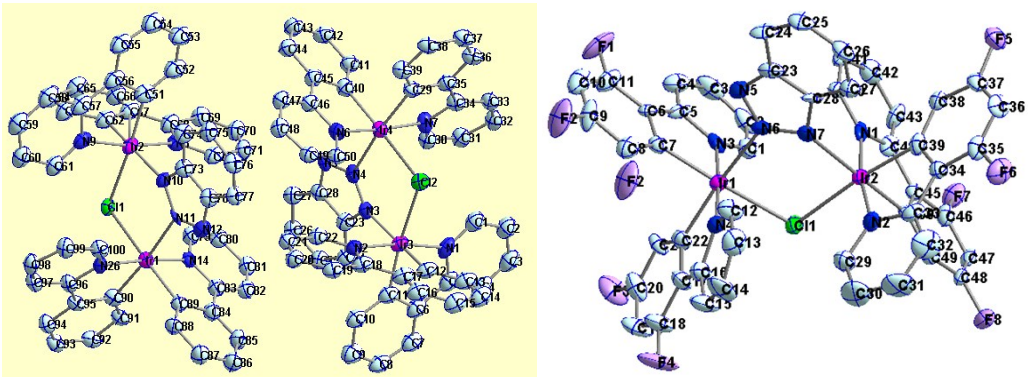

Complex 1 **Complex 2**

Figure S1 Oak Ride Thermal Ellipsoidal Plot (*ORTEP*) diagram of complex **1** and **2**. All hydrogen atoms have been omitted for clarity.

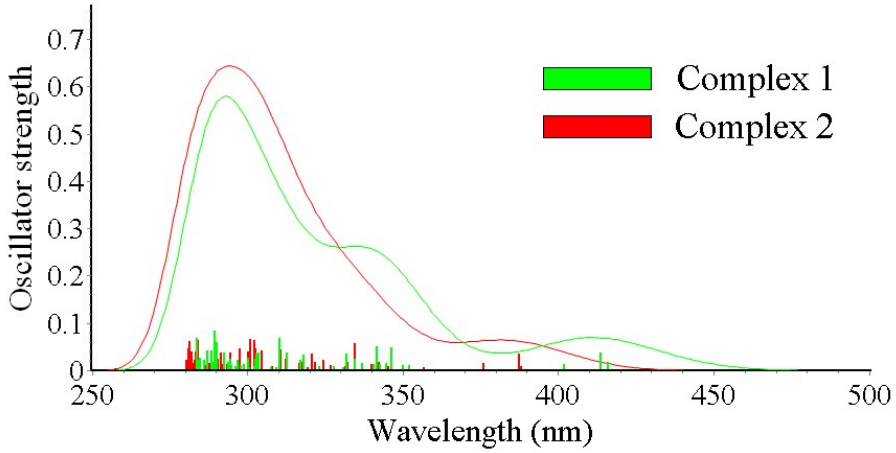

Figure S2 the calculated absorption spectra of complex **1** and complex **2**

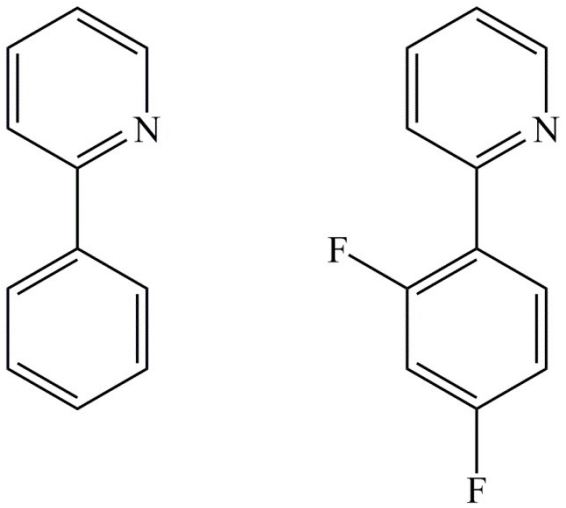

Figure S3 The constitutional formula of C^N of complex **1** and complex **2**

Table S1 Crystal Data Collection and Refinement Details for complex **1** and complex **2.**

	Complex 1	**Complex 2**
Formula	$C_{50}H_{36}ClIr_2N_7$	$C_{50}H_{28}ClF_8Ir_2N_7$
Mr	1154.75	1298.69
Cryst. Size, mm^3	0.36 x 0.3 x 0.29	0.24 x 0.18 x 0.16
Crystal system	Monoclinic	Triclinic
space group	P21/c	P-1
a, Å	15.496	10.534
b, Å	20.271	15.315
c, Å	33.729	16.045
α, deg		80.638
β, deg	94.887	86.499
γ, deg		78.116
Z	4	2
D_{calcd}, g cm^{-3}	1.452	1.726
F(000), e	4444.0	1240.0
hkl range	-12<=h<=18	-12<=h<=9
	-24<=k<=23	-16<=k<=18
	-40<=l<=40	-18<=l<=19
ϑ range, deg	1.17 – 25.11	1.29 – 25.05
Reflections collected/ unique	53004 / 18810	12747 / 8710
	[R(int) = 0.0572]	[R(int) = 0.0394]
Data / parameters	18810 / 1081	8710 / 613
GoF (F^2)	1.024	1.013
R_1/wR_2 [$I > 2\sigma(I)$]	0.0539 / 0.1487	0.0456 / 0.0994
R_1/wR_2 (all data)	0.0841 / 0.1589	0.0745/ 0.1059
Largest diff. peak/hole/e $Å^{-3}$	1.84 / -3.91	1.373 / -1.114
CCDC no.	890422	890423

Table S2 A detailed elucidation of the electron density plots of the HOMO and the LUMO for **[{Ir(ppy)$_2$Cl}$_2$], [{Ir(dfppy)$_2$Cl}$_2$], [{Ir(ppy)$_2$}$_2$Cl(BTA)]** and **[{Ir(dfppy)$_2$}$_2$Cl(BTA)]**.

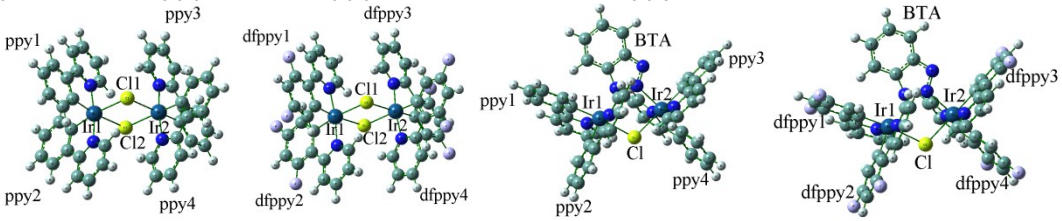

{Ir(ppy)$_2$Cl}$_2$(a) **{Ir(dfppy)$_2$Cl}$_2$(b)** **{Ir(ppy)$_2$}$_2$Cl(BTA) (1)** **{Ir(dfppy)$_2$}$_2$Cl(BTA) (2)**

		Ir1	Ir2	Cl	BTA	ppy1/dfppy1	ppy2/dfppy2	ppy3/dfppy3	ppy4/dfppy4
a	HOMO	25%	25%	6%		11%	11%	11%	11%
	LUMO	2%	3%			22%	22%	24%	24%
b	HOMO	25%	25%	6%		11%	11%	11%	11%
	LUMO	7%	7%	4%		20%	20%	21%	21%
1	HOMO	3%	50%	1%	1%		2%	23%	18%
	LUMO	6%	2%	2%		26%	60%	2%	2%
2	HOMO	3%	47%	2%	1%	2%	1%	25%	19%
	LUMO	6%	2%	2%		18%	64%	2%	5%

Table S3 The computed and experimental emission spectra of complex **1** and **2** in CH_2Cl_2 solution, and the results of the emissive assignments.

	λ(nm)(computl/exptl)	Major configuration	Character
1	477.93/484	L→H(57%)	ppy1/ppy2→Ir2/ppy3/ppy4(MLCT/LRET)
2	474.90/478	L→H(60%)	dfppy1/dfppy2→Ir2/dfppy3/dfppy4(MLCT/LRET)

Table S4 The quantum yield (*Q*) of samples was calculated with the following equation. Quinine sulfate in 0.1 M H_2SO_4 (literature quantum yield 54% at 360 nm) was chose as a standard. Since *Q* is the quantum yield, *I* is the measured integrated emission intensity, *n* is the refractive index, and *A* is the optical density. The subscript *R* refers to the reference fluorophore of known quantum yield.

samples	Intergrated emission intensity (*I*)	Abs. At 360nm *(A)*	Refractive index of solvent (*n*)	Quantum yield at 360nm (*Q)*
Quinine sulfate	448333	0.09	1.33	54%
1	10977	0.136	1.42	1%
2	19509	0.105	1.42	2.3%

Reference:

1. M. Song, Z. Hao, Z. Wu, S. Song, L. Zhou, R. Deng and H. Zhang, *International Journal of Quantum Chemistry*, 2013, **113**, 1641.
2. M. Song, Z. Hao, Z. Wu, S. Song, L. Zhou, R. Deng and H. Zhang, *J. Phys. Org. Chem.,* 2013, **26**, 840.
3. M. Song, G. Wang, J. Wang, Y. Wang, F. Bai and Z. Qin, *Spectrochimica Acta Part A: Molecular and Biomolecular Spectroscopy*, 2015, **134**, 406.
4. M. Song, J. Huang, F. Bai, C. Wang, H. Liu, J. Wang, D. Li and Z. Qin, *Chem. Res. Chin. Univ.*, 2016, **32**, 451.
5. M. J. Frisch, G. W. Trucks, H. B. Schlegel, G. E. Scuseria, M. A. Robb, J. R. Cheeseman, G. Scalmani, V. Barone, B. Mennucci, G. A. Petersson, H. Nakatsuji, M. Caricato, X. Li, H. P. Hratchian, A. F. Izmaylov, J. Bloino, G. Zheng, J. L. Sonnenberg, M. Hada, M. Ehara, K. Toyota, R. Fukuda, J. Hasegawa, M. Ishida, T. Nakajima, Y. Honda, O. Kitao, H. Nakai, T. Vreven, J. A. Montgomery Jr., J. E. Peralta, F. Ogliaro, M. J. Bearpark, J. Heyd, E. N. Brothers, K. N. Kudin, V. N. Staroverov, R. Kobayashi, J. Normand, K. Raghavachari, A. P. Rendell, J. C. Burant, S. S. Iyengar, J. Tomasi, M. Cossi, N. Rega, N. J. Millam, M. Klene, J. E. Knox, J. B. Cross, V. Bakken, C. Adamo, J. Jaramillo, R. Gomperts, R. E. Stratmann, O. Yazyev, A. J. Austin, R. Cammi, C. Pomelli, J. W. Ochterski, R. L. Martin, K. Morokuma, V. G. Zakrzewski, G. A. Voth, P. Salvador, J. J. Dannenberg, S. Dapprich, A. D. Daniels, Ö. Farkas, J. B. Foresman, J. V. Ortiz, J. Cioslowski and D. J. Fox, *Gaussian 09 Revision D.01*, (2009) Gaussian, Inc., Wallingford, CT, USA.